RACK1 cooperates with NRASQ61K to promote melanoma in vivo

Cécile Campagne, Edouard Reyes-Gomez, M.E. Picco, Sophia Loiodice, Paul Salaun, Jacky Ezagal, Florence Bernex, P.H. Commere, Stéphanie Pons, Diane Esquerre, et al.

Contents lists available at ScienceDirect

Cellular Signalling

journal homepage: www.elsevier.com

RACK1 cooperates with *NRAS*^{Q61K} to promote melanoma *in vivo*

C. Campagne[a, b, *], E. Reyes-Gomez[a, b, c], M.E. Picco[d], S. Loiodice[a, b, 1], P. Salaun[a, b], J. Ezagal[a, b], F. Bernex[a, b, c, 2], P.H. Commère[e], S. Pons[f], D. Esquerre[g], E. Bourneuf[h, i], J. Estellé[h], U. Maskos[f], P. Lopez-Bergami[d, j], G. Aubin-Houzelstein[a, b], J.J. Panthier[a, b, k, l], &G. Egidy[a, b, h, **]

[a] *INRA, UMR955 Génétique Fonctionnelle et Médicale, Ecole Nationale Vétérinaire d'Alfort, F-94704 Maisons-Alfort, France*
[b] *Université Paris-Est, Ecole Nationale Vétérinaire d'Alfort, UMR955 Génétique Fonctionnelle et Médicale, F-94704 Maisons-Alfort, France*
[c] *Université Paris-Est, Ecole Nationale Vétérinaire d'Alfort, Unité d'Embryologie, d'Histologie et d'Anatomie Pathologique, F-94704 Maisons-Alfort, France*
[d] *Instituto de Medicina y Biologia Experimental, CONICET, Buenos Aires, Argentina*
[e] *Plateforme de Cytométrie, Département d'Immunologie, Institut Pasteur, F-75724 Paris, France*
[f] *Unité Neurobiologie Intégrative des Systèmes Cholinergiques, UMR 3571, CNRS, Institut Pasteur, F75724 Paris Cedex 15, France*
[g] *GenPhySE, Université de Toulouse, INRA, INPT, ENVT, Castanet Tolosan, France*
[h] *GABI, INRA, AgroParisTech, Université Paris-Saclay, Jouy-en-Josas, France*
[i] *LREG, CEA, Université Paris-Saclay, F-78352 Jouy-en-Josas, France*
[j] *Centro de Estudios Biomédicos, Biotecnologicos, Ambientales y Diagnostico, Universidad Malmonides, CONICET, Buenos Aires, Argentina*
[k] *CNRS URM 3738, USC INRA 2026, F-75724, France*
[l] *Institut Pasteur, Département de Biologie du Développement et Cellules Souches, Génétique fonctionnelle de la Souris, 25 rue du Docteur Roux, Paris F-75724, France*

ARTICLE INFO

Keywords:
Scaffold
MAPK pathways
Melanocyte
JNK
STAT3
Angiogenesis

ABSTRACT

Melanoma is the deadliest skin cancer. RACK1 (Receptor for activated protein kinase C) protein was proposed as a biological marker of melanoma in human and domestic animal species harboring spontaneous melanomas. As a scaffold protein, RACK1 is able to coordinate the interaction of key signaling molecules implicated in both physiological cellular functions and tumorigenesis. A role for RACK1 in rewiring ERK and JNK signaling pathways in melanoma cell lines had been proposed. Here, we used a genetic approach to test this hypothesis *in vivo* in the mouse. We show that *Rack1* knock-down in the mouse melanoma cell line B16 reduces invasiveness and induces cell differentiation. We have developed the first mouse model for RACK1 gain of function, *Tyr::Rack1-HA* transgenic mice, targeting RACK1 to melanocytes *in vivo*. RACK1 overexpression was not sufficient to initiate melanomas despite activated ERK and AKT. However, in a context of melanoma predisposition, RACK1 overexpression reduced latency and increased incidence and metastatic rate. In primary melanoma cells from *Tyr::Rack1-HA*, *Tyr::NRas*^{Q61K} mice, activated JNK (c-Jun N-terminal kinase) and activated STAT3 (signal transducer and activator of transcription 3) acted as RACK1 oncogenic partners in tumoral progression. A sequential and coordinated activation of ERK, JNK and STAT3 with RACK1 is shown to accelerate aggressive melanoma development *in vivo*.

1. Introduction

Cutaneous melanoma is the deadliest skin cancer. Melanoma has a high metastatic capacity. Despite recent clinical breakthroughs, the majority of metastatic melanoma patients do not survive [1]. The study of a minipig melanoma model revealed an overexpression of *RACK1* (Receptor for activated protein kinase C) mRNA in melanoma cells [2]. RACK1 protein is strongly expressed in melanoma cells of primary tumors and metastases in different mammalian species: patients [2], horses [3] and dogs [4]. In sharp contrast, RACK1 is not detected in normal skin melanocytes or in nævi by immunofluorescence [2–4]. Interestingly, RACK1 increased the survival of human melanoma MeWo cells following UV induced-apoptosis. Moreover, inhibition of RACK1 expression using RNA interference was shown to reduce the tumorigenicity of MeWo cells in a xenograft model [5].

* Correspondence to: C. Campagne, INRA, UMR955 Génétique Fonctionnelle et Médicale, Ecole Nationale Vétérinaire d'Alfort, F-94704 Maisons-Alfort, France.
** Correspondence to: G. Egidy, GABI, INRA, AgroParisTech, Université Paris-Saclay, 78350 Jouy-en-Josas, France.
Email addresses: cecile.campagne@curie.fr (C. Campagne); giorgia.egidy-maskos@inra.fr (G. Egidy)
1 Current address: Laboratoire de Physiopathologie Orale et Moléculaire, Centre de Recherche des Cordeliers, INSERM UMR1138, F-75006 Paris, France.
2 Current address: RHEM - Institut de Recherche en Cancérologie de Montpellier, INSERM U896, F-34298 Montpellier, France.

http://dx.doi.org/10.1016/j.cellsig.2017.03.015
Received 30 December 2016; Received in revised form 20 March 2017; Accepted 22 March 2017
Available online xxx
0898-6568/

RACK1 is a ubiquitous and abundant protein [6]. It is a scaffold containing seven WD40 repeats considered protein-protein interaction platforms. Through its ability to coordinate the interaction of key signaling molecules, RACK1 is thought to integrate various pathways involved in both physiological and tumorigenic cellular functions making it a signaling hub [7]. Yet, the extent to which the multiple binding partners of RACK1 are coordinated has not been much tested *in vivo*. In an attempt to alter RACK1 levels in mammals, the group of S. Biffo obtained one mouse line with a hypomorphic *Rack1* allele. While homozygosity for that hypomorphic *Rack1* allele resulted in a lethal phenotype, heterozygous adult mice showed no major phenotype except for a belly spot and hypopigmented tail and paws [8], typical features of a developmental defect in melanoblast migration.

A role for RACK1 in the crosstalk between ERK (Extracellular signal-regulated kinase) and JNK (c-Jun N-terminal kinase) signaling in melanoma was proposed to set up a feed forward mechanism triggering tumoral progression [9]. In the light of these *in vitro* data, we hypothesized that gain of function of RACK1 targeted to melanocytes in the context of *NRas* constitutive activation would accelerate melanomagenesis by strengthening converging tumoral signaling.

As for other solid cancers, cutaneous melanoma development is considered as a multistep process. Melanomagenesis requires a combination of gain of function mutations in oncogenes and loss of function mutations in tumor suppressor genes [10]. The first spontaneous metastasizing melanoma model harbored the $NRas^{Q61K}$ mutation in a deleted *Cdkn2a* background [11]. To test whether an overexpression of RACK1 was sufficient to trigger melanoma, we created *Tyr::Rack1-HA* transgenic mice in which a hemaglutinin (HA) epitope-tagged-RACK1 is expressed off the *Tyrosinase* promoter. We show here that RACK1 overexpression is not sufficient to trigger nevi or melanomas despite ERK and AKT activation. Yet, in a context of melanoma predisposition, RACK1 melanocytic overexpression reduced latency and increased incidence and metastatic rate. We found activated JNK and STAT3 as partners of RACK1 in melanomagenesis.

2. Materials and methods

2.1. Mice and genotyping

Mouse *Rack1* cDNA was tagged with HA by PCR before insertion in a pBSK-UPT-Tyr-SV40 plasmid [12]. Micro-injection of the linearized vector was made in B6CBAF1/J fertilized oocytes. *Tyr::Rack1-HA* transgenic founders were characterized by Southern blot analysis and PCR genotyping. Data come from the 7th backcross onwards on C57BL/6J background. The $Pax3^{GFP}$ and -*Cdkn2a* alleles and $Tyr::NRas^{Q61K}$ transgene have been backcrossed onto the C57BL/6J background for > 15 generations [13]. Animal care and use for this study were approved by the ethical board of Alfort Veterinary School in accordance with European Union Standards (agreement number 16, notice 14/02/12-4). To identify the *Tyr::Rack1-HA* transgene, the following primers were used: forward: 5′-gtcgacatgaccgagcagatgacc-3′ and reverse 5′-tacatggttgcgccatctgcgccgcgggtaccaatag-3′. PCR conditions were 30 s at 94 °C, 30 s at 65 °C, 30 s at 72 °C for 30 cycles and a final extension step at 72 °C for 10 min. The other genotyping conditions were as described [13].

2.2. Histologic analysis and immunofluorescence in mouse samples

Complete necropsy and systematic pathological analysis were performed on all mice as described [14]. Immunofluorescence was performed with mouse monoclonal anti-RACK1 (Transduction Laboratories, dilution 1:150, BD Biosciences, Le Pont de Claix, France), chicken polyclonal anti-GFP (Abcam, 1:600, Paris, France), mouse monoclonal anti-HA (Covance, 1:600, Rueil-Malmaison, France), rabbit anti-cytokeratin5 (Thermo Scientific, 1:100, Fisher Scientific, Illkirch, France) and rabbit polyclonal anti-pERK (Thr202/Tyr204, 1:200) and anti-pAKT (Ser473, 1:50) (Cell Signaling, Ozyme, St Quentin, France) and rabbit anti-ERK 1:100, goat anti-Ki67 1:100, anti-STAT3, anti-JNK (D-2) (Santa Cruz, Heidelberg Germany) antibodies. Nuclear counter-staining was achieved with 4′,6′-diamidino-2-phenylindole (DAPI) (1:1000, Invitrogen). Sections were examined with a Zeiss Axio Observer Z1M ApoTome microscope (Carl Zeiss S.A.S., Le Pecq, France). Controls without the first antibodies showed no unspecific labeling. Images were processed with the *AxioVision* computer program version 4.6 (Carl Zeiss). Figures are representative of the skin samples evaluated (n > 8 for each mouse line). All images shown are individual sections of z series stack. Final figures were assembled with Adobe Photoshop CS3 (Adobe Systems; USA). Quantification of Ki67/GFP positive nuclei was performed on images obtained at 40 × in regions positive for Ki67, counting at least 30 GFP^+ cells per field, 2 fields per mouse, 6 mice per genotype.

2.3. Fluorescent activated cell sorting (FACS), cell culture, soft agar assays and immunofluorescence

Skin melanocytes and melanoma cells from primary tumors (n = 6) or metastases (lymph nodes n = 6; lung n = 4; liver n = 1; brain n = 1) were isolated, FACS-sorted and cultured as previously described [13]. B16 melanoma cell line was grown in DMEM medium with 10% fetal calf serum and penicillin/streptomycin. All cells were grown at 37 °C under 5% CO_2 at pH 7.0–7.1. ERK inhibitor U0126, 5 μM and 10 μM, and JNK inhibitor SP600126 20 μM (Sigma-Aldrich, Saint-Quentin Fallavier, France) were incubated for 24 or 48 h. Human cells UACC903 were cultured as previously described [9]. Soft agar tests were made in 96-well plates as described [13].

For immunofluorescence on cells plated onto coverslips, fixation lasted 15 min in 2% PFA and permeabilization with ice-cold methanol, 10 min. Immunolabeling on cells or agar slices was performed like in tissue section with the omission of the antigen retrieval step. Antibodies used were mouse monoclonal anti-Ki67 (1:100, Novocastra, Newcastle upon Tyne, UK), rabbit polyclonal anti-pPKCα/β_{II} (Thr638/641, 1:100), anti-pJNK (pSAPK Thr183/Tyr185, 1:25), anti-pSTAT3 (Tyr705, 1:100) (Cell Signaling) and as above.

2.4. RNA interference and transduction

Mouse *Rack1* shRNA sequence (ID# 61854) corresponding to a sequence inside exon 2, was obtained from Ambion (Invitrogen): GGTCACTCCCACTTCGTTATT and the scramble sequence used was GTCACTCACCCTTCGGTTATT [15]. Lentiviral vectors with GFP reporter of infections were produced as previously described [16]. Three *Stat3* shRNA (ID# 424803, 424802, 641819) were obtained from Open Biosystem (Thermo Fisher Scientific) as lentiviral vectors. Transduction was performed with at 0.45 ng/μl of lentiviral titer in presence of polybrene. RNA was collected on the third day.

2.5. RNA extraction and quantitative RT-PCR

RNA extractions were performed on 20,000 FACS-sorted cells following RNA XS kit manufacturer instructions (Macherey Nagel, Germany) as described [13]. RNA sequencing (RNA-seq) on *shScramble* and *shRack1*-treated melanocytes, primary melanoma from *Tyr::NRas*; Pax3*$^{GFP/+}$ cells with or without *Tyr::Rack1-HA* was performed on technical triplicates of viral infection. Libraries were prepared by selecting polyadenylated mRNA using the TruSeq RNA Sample Prep Kit (Illumina, San Diego, CA). When performed on plated infected cells, RNA was prepared from 10^6 cells in 6 well plates. qPCR assays on cDNA from primary cells infected with *shRack1* were performed using TATAA Granscript cDNA Supermix for reverse transcription and TATAA SYBR

GranMaster mix on a Light Cycler480 qPCR instrument (Roche) (TATAA Biocenter, Czech Republic). *Actb*, *Gapdh*, *Tubb5* and *Rnp2* were used as reference genes. Experiments were carried out at least twice in triplicates.

2.6. Protein extractions, immunoprecipitation, Western-blot analyses and JNK kinase assay

Experiments were performed as described [13], at least twice. Antibodies used were anti-tubulin (Cell Signaling), anti-STAT3, anti-JNK (D-2) (Santa Cruz, Heidelberg Germany) and the same as above. JNK immunokinase assays were performed with endogenous JNK as previously described [5].

2.7. Statistical methods

Error bars in the figures represent standard errors of the mean. The two-tailed Student's *t*-test or nonparametric Mann-Whitney *U* test were used to assess differences between groups. A *P*-value < 0.05 was considered as statistically significant (***$P < 0.001$, **$P < 0.01$).

Other details regarding transgenesis construct, histological analysis, immunofluorescence in skin samples and cells, RNA interference and transduction, quantitative RT-PCR, RNA seq or Western blot are available in the supplementary section.

3. Results

3.1. Effect of RACK1 knock-down on metastatic melanoma cell clonogenicity and differentiation

To test the importance of RACK1 in melanoma development we developed a *Rack1* shRNA lentivirus by inserting a previously validated sequence [15] into a backbone allowing visual control of infection [16] (Fig. 1a). The murine melan-a cell line, which is a nontransformed immortalized melanocytic line, and the highly metastatic B16 melanoma line were used to test RACK1 knock-down. With a transduction efficacy around 90%, RACK1 protein was efficiently reduced by sh*Rack1* as evaluated by immunofluorescence and Western blot analyses without affecting unrelated proteins like Tubulin, three days post transduction of metastatic B16 cells (Fig. 1a). However, B16-sh*Rack1* cells were pro-

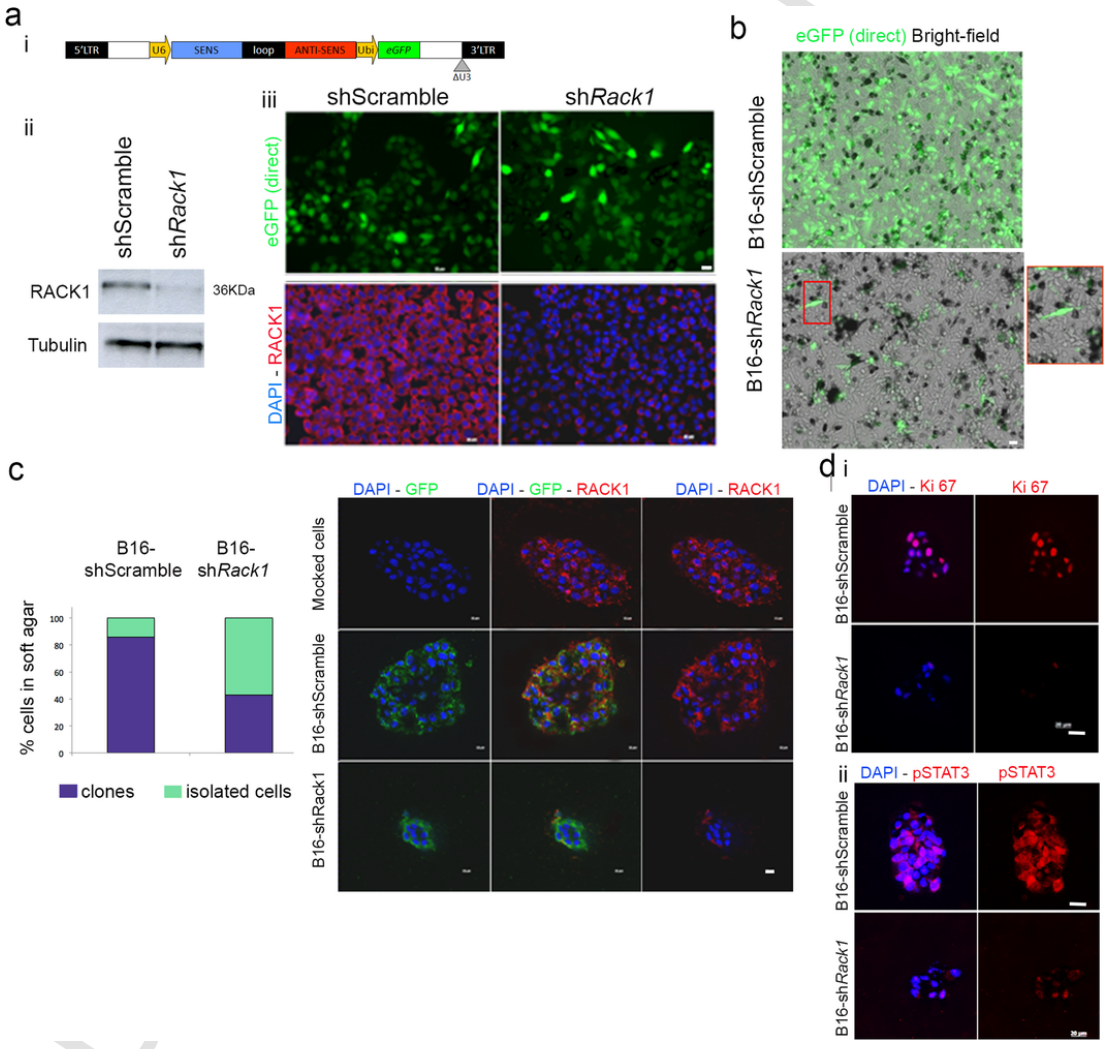

Fig. 1. RACK1 knock-down reduced B16 melanoma cells invasiveness and led to cell differentiation.a: i Lentiviral vector backbone for shRNA expression with GFP control of transduction; ii Western-blot analysis for RACK1 and Tubulin in *shRack1* and *shScramble* B16 cells 3 days post-transduction (3dpt); iii Fluorescent microscopy analysis of direct GFP signal (green) and immunolabeling for RACK1 (red) on 3 day-transducted cells. b: Aspect of *shRack1* and *shScramble*-treated B16 cultures 14 days after transduction. Note the differentiation and loss of GFP^+ cells in *shRack1*-treatd B16 cells. c: Soft agar assay of *shRack1* and *shScramble*-treated B16 cells 3dpt, i Proportions of clones (purple) and isolated cells that did not proliferate (green); ii Immunolabeling for GFP (green) and RACK1 (red) in B16 clones mock-treated or treated with *shRack1* or *shScramble*; d: Immunolabeling for i) the proliferation marker Ki67 (red) or ii) pSTAT3 (red) on soft agar clones. Nuclear counterstaining with DAPI (blue). Bars: 20 μm. (For interpretation of the references to colour in this figure legend, the reader is referred to the web version of this article.)

gressively lost from day 10 to day 20 post transduction, being replaced by cells not transduced, hence not expressing the shRNA (Fig. 1b). Remaining fluorescent B16-sh*Rack1* cells showed a differentiated phenotype. They switched from the typical rounded B16 shape to a melanocyte-like shape with dendritic extensions and higher melanin content (Fig. 1b), as did melan-a cells (Fig. S1).

We assessed the effect of RACK1 silencing on anchorage-independent cell growth of 3 day transduced cells. Only 40% of B16-sh*Rack1* cells formed clones in soft agar compared to 86 and 88% in B16-sh*Scramble* and B16-mock cells, respectively (χ^2 test; $P < 0{,}0005$) (Fig. 1c). Furthermore, the B16-sh*Rack1* clones were smaller than the controls (Fig. 1c). This reduced size of B16-sh*Rack1* clones relates to a sharp reduction of Ki67 and pSTAT3 staining (Fig. 1d).

3.2. Overexpressed RACK1 in melanocytic cells from the Tyr::NRas^{Q61K} melanoma model

We next determined RACK1 expression in the *Tyr::NRas^{Q61K}; Cdkn2a$^{-/-}$* mouse melanoma model, referred to as *Tyr::NRas** thereafter. These mice carry a melanocyte-targeted *NRas^{Q61K}* transgene which leads to constitutive ERK activation [11]. *Tyr::NRas** mice develop early dermal melanocytic proliferation responsible for skin hyperpigmentation, which can eventually progress to a malignant lesion [14]. We have shown that introduction of the *Pax3^{GFP}* allele allows the identification of fluorescent melanocytic cells in the skin without affecting melanoma development [13,17]. Immunofluorescence on cutaneous melanomas showed a cytoplasmic RACK1 signal in GFP$^+$ cells (Fig. 2a). RACK1 was immunodetected in all lesions from *Tyr::NRas*; Pax3$^{GFP/+}$* and *Tyr::NRas** mice.

We also tested melanoma-free skin. In control *Pax3$^{GFP/+}$; Cdkn2a$^{-/-}$* mice, RACK1 protein was highly expressed in the cytoplasm of keratinocytes, here considered as positive controls. In contrast, melanocytes identified as GFP$^+$ cells were negative for RACK1. We excluded the possibility that melanocytes displayed membrane RACK1 signal with triple immunostaining against RACK1, GFP and cytokeratin 5 (CK5), a marker of basal keratinocytes. Instead, in *Tyr::NRas*; Pax3$^{GFP/+}$* mice, skin sections displayed a specific cytoplasmic RACK1 signal in GFP$^+$, CK5$^-$ melanocytes (Fig. 2b). Follicular, interfollicular and dermal melanocytes displayed this specific melanocytic RACK1 signal (Fig. S2). To test whether RACK1 overexpression occurred at the transcript level, GFP$^+$ melanocytes were sorted by FACS from neonatal skins. Higher *Rack1* mRNA levels were observed in *Tyr::NRas*; Pax3$^{GFP/+}$* melanocytes isolated from neonatal skin compared to *Cdkn2a$^{-/-}$; Pax3$^{GFP/+}$* control pup littermates (Fig. 2c). Thus, ERK activation together with RACK1 overexpression is associated with melanoma and melanoma predisposition in this model.

To study signaling associated with the progression stages, we established primary cultures from neonatal skin, primary tumor, locoregional metastasis, and distant metastasis which, as expected, were pERK$^+$ according to *NRas^{Q61K}* expression when assayed by immunofluorescence and Western blot (Fig. 2d) [13]. In these cells, overexpression of *Rack1* mRNA (Fig. 2e) and high RACK1 protein level were identified (Fig. 2f). Interestingly, a 60 kDa band in addition to the predicted 36 kDa band was revealed in tumor cells compared to melanocytes (Fig. 2f). Denaturing conditions did not support dimerization of RACK1 (not shown). Inhibition of MEK1 with U0126 did not alter RACK1 reactivity in melanoma cells (Fig. S3).

3.3. Activated ERK and transiently increased skin melanocytes in pups with Rack1 gain of function in melanocytes

To address a causative role of RACK1 in melanoma development, we generated *Tyr::Rack1-HA* transgenic mice. We used the 6.1 kb promoter sequence of the mouse *Tyrosinase* gene in combination with the 3.6 kb distal control region [12] to target the expression of the mouse *Rack1* gene (MGI:101849) that encodes RACK1, tagged by HA, to the melanocytic lineage (Fig. 3a). RACK1-HA expression from the *Tyr::Rack1-HA* transgene was detected when transfected into B16 cells *in vitro* (Fig. 3a).

Five *Tyr::Rack1-HA* transgenic founders were obtained using classical transgenesis (Fig. 3aiii). All founders were viable, fertile and reached adulthood without displaying any overt phenotype. Three lines were established with offspring from three distinct founders and analysed in detail. In order to easily identify melanocytes, the three lines were crossed with *Pax3$^{GFP/+}$* mice. Melanocytes were FACS-sorted on GFP from back skin of 3 day-old pups for each transgenic line and quantitative RT-PCR assays were performed. As expected, *Rack1* mRNA levels in melanocytes were higher in *Tyr::Rack1-HA; Pax3$^{GFP/+}$* mice than in *Pax3$^{GFP/+}$* littermates in each transgenic line (Fig. 3b). *Rack1/Actb* ratios were comparable to ratios measured in the *Tyr::NRas** mice.

Protein expression of RACK1 in melanocytes in furry and glabrous skin was assessed by immunofluorescence (Fig. 3c, Fig. S4). In *Tyr::Rack1-HA; Pax3$^{GFP/+}$* melanocytes, GFP and HA protein signals were colocalized (Fig. 3c, third line). Moreover, a specific cytoplasmic RACK1 signal was detected in GFP and HA-positive melanocytes (Fig. 3c). Triple immunostaining against RACK1, GFP and CK5 confirmed the melanocytic origin of the RACK1 signal (Fig. 3c, fourth line). Thus, in our three *Tyr::Rack1-HA* transgenic mouse lines, *Rack1* mRNA was overexpressed and RACK1 protein was detected in melanocytes. This excluded a role of the integration site of the transgene.

RACK1 was reported to associate with the core kinases of the ERK pathway and RACK1 reduction resulted in lower ERK activity while RACK1 overexpression produced an increased ERK activation [18,19]. We tested ERK activation in melanocytes of transgenic *Tyr::Rack1-HA; Pax3$^{GFP/+}$* and *Pax3$^{GFP/+}$* control mice by immunostaining (Fig. 3d). In control *Pax3$^{GFP/+}$* melanocytes, pERK signal was hardly detected. Instead, in *Tyr::Rack1-HA; Pax3$^{GFP/+}$* melanocytes, nuclear GFP and pERK signals were co-localized. Besides, pERK signal was also identified in keratinocytes. Noteworthy, total ERK expression was equivalent in both sample types (Fig. S5). We checked whether the PI3K/AKT pathway was also activated in the skin of *Tyr::Rack1-HA* transgenics. Nuclear pAKT signal was detected as well as in *Tyr::NRas*, Pax3$^{GFP/+}$* skins, as opposed to *Pax3$^{GFP/+}$* skin (not shown). These data suggest that RACK1 overexpression associated with ERK and AKT activation. We studied whether this pERK immunodetection corresponded to a proliferative signal translating efficient ERK activation. *Tyr::Rack1-HA; Pax3$^{GFP/+}$* skin biopsies presented 26% more GFP$^+$ cells than *Pax3$^{GFP/+}$* skins (Fig. 3e). Yet, no coat or skin hyperpigmentation was visible in any of the mouse lines. Over 17 months of follow-up, no melanocytic lesions were detected in any of the three transgenic lines ($n > 15$ mice/line). In addition, the morphology of the skin was normal indicating that RACK1 overexpression alone was not sufficient to drive melanoma development (Fig. S6).

3.4. Accelerated melanoma appearance with RACK1-HA expression in a context of Tyr::NRas* melanoma predisposition

Melanoma penetrance is not complete in the *Tyr::NRas** model [11]. In our colony, 33% of mice develop melanoma [14]. To assess the effects of RACK1 expression in a genetic background predisposing to melanoma, we produced *Tyr::Rack1-HA; Tyr::NRas*; Pax3$^{GFP/+}$* mice for the three *Tyr::Rack1-HA* independent transgenic lines. These mice developed melanocytic lesions ranging from benign to malignant tumors [14] (Fig. 4a). No differences in latency and incidence were seen between the three transgenic lines. Nevertheless, 78% of the *Tyr::Rack1-HA; Tyr::NRas*;Pax3$^{GFP/+}$* mice in each line showed reduced latency within about 10 months, mean 7.5 months (Mann-Whitney test; $P < 0.002$) (Fig. 4b). Besides, 55% of mice developed

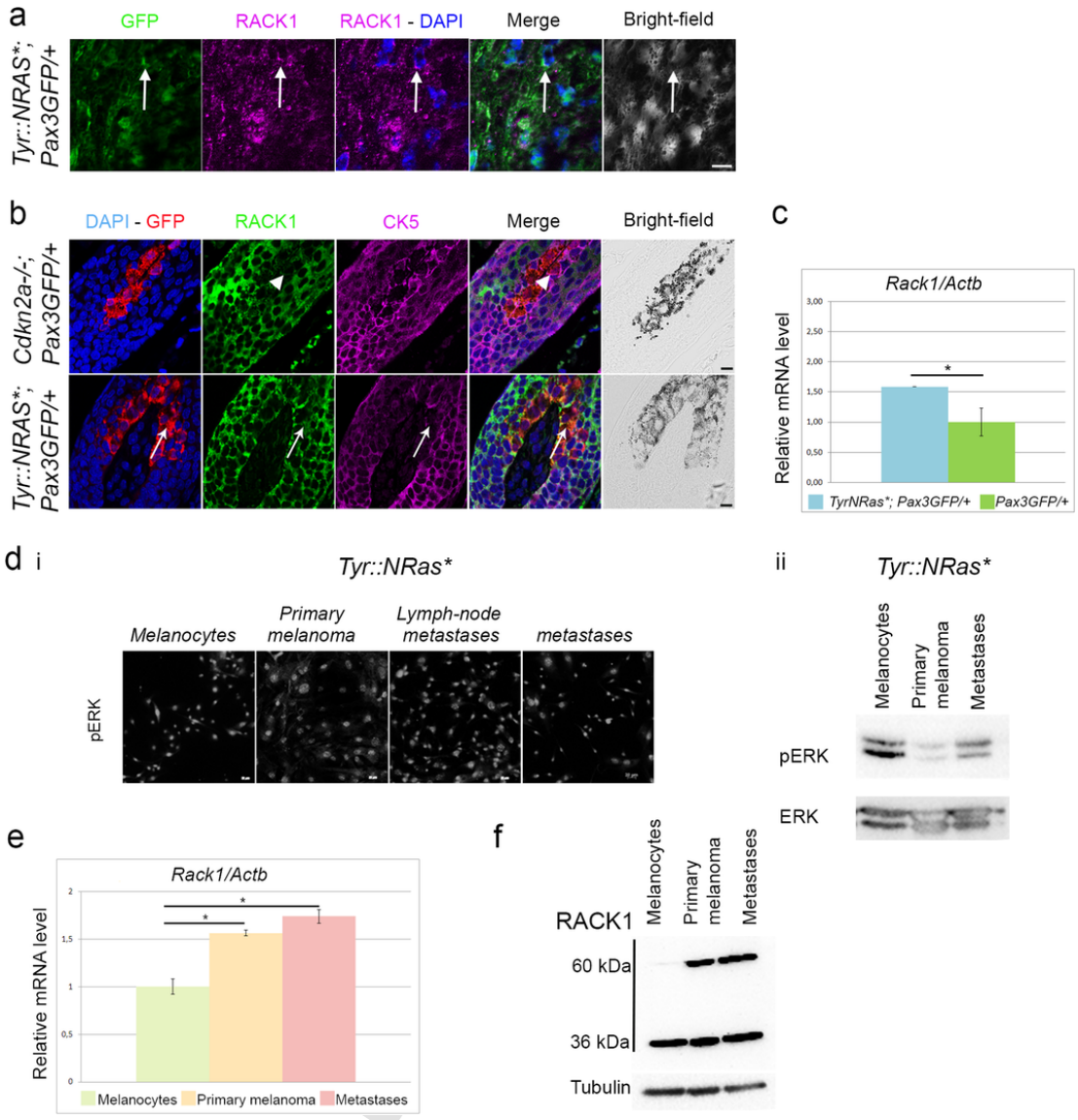

Fig. 2. The *Tyr::NRas*, Pax3*$^{GFP/+}$ mouse melanoma model displays increased RACK1 in hyperplastic melanocytes.ApoTome microscopy analysis of triple labeling for GFP, RACK1 and CK5 in melanoma (a) and dorsal skin from *Tyr::NRas* Pax3*$^{GFP/+}$ and control *Cdkn2a*$^{-/-}$*; Pax3*$^{GFP/+}$ mice (b). GFP (green), RACK1 (magenta) in a; GFP (red), RACK1 (green) and CK5 (magenta) in b. Arrows point to melanoma cells or melanocytes with RACK1 signal. Arrowheads point to melanocytes without RACK1 signal. DAPI nuclear counterstaining in blue. Bars: 10 μm. c: Reverse transcription-qPCR for *Rack1* mRNA in melanocytes isolated from *Tyr::NRas*, Pax3*$^{GFP/+}$ (n = 5) mice compared to control *Pax3*$^{GFP/+}$ (n = 5). Results shown are *Rack1* expression normalized to *Actb*. d: i: pERK immunolabeling in GFP-FACS sorted cells from neonatal skin and cutaneous melanomas at different progression stages in *Tyr::NRas*, Pax3*$^{GFP/+}$ mice. ii: Western blot of pERK and ERK on the same cells as in i. e: Quantitative RT-PCR for *Rack1* mRNA in GFP$^+$ sorted melanocytic cells from skin, primary melanoma and metastases in *Tyr::NRas*; Pax3*$^{GFP/+}$ normalized to *Actb* from triplicates. f: Western-blot analysis for RACK1 in GFP + sorted cells as in e. Note a 60 kDa band specific to tumoral cells on top of the 36 kDa expected band. * $P < 0.05$. (For interpretation of the references to colour in this figure legend, the reader is referred to the web version of this article.)

melanomas, indicating a clear increase in incidence of primary cutaneous malignant lesions (n = 22/31, χ^2 test; $P < 0.05$) (Fig. 4a). Moreover, distant metastases were more frequently identified in *Tyr::Rack1-HA; Tyr::NRas*; Pax3*$^{GFP/+}$ mice (55%, n = 12/22) compared to *Tyr::NRas*; Pax3*$^{GFP/+}$ mice (36%, n = 9/25) (Fig. 4c). Histological analysis of the lesions detected no differences between *Tyr::Rack1-HA* lesions and those of control *Tyr::NRas*; Pax3*$^{GFP/+}$ littermates (Fig. 4a). However, when the proliferation status of melanocytic cells was analysed using Ki67 labeling, *Tyr::Rack1-HA* bearing melanomas presented a higher index than controls (Fig. 4d) (32.9 ± 17.8 *versus* 22.3 ± 8.1 respectively, Student's *t*-test; $P < 0.05$).

The higher incidence, lower latency and higher frequency of mitosis provide the first *in vivo* evidence of a contribution of RACK1 to melanoma development. Histological data point to an acceleration of the proliferative status of the lesions.

3.5. JNK and STAT3 as oncogenic partners of RACK1 in melanoma development

To investigate the clinical advantage conferred by the overexpression of RACK1 in the *Tyr::NRas** model, we explored candidate proteins related to metastasis. STAT3 activation has been shown to promote metastasis in melanoma [20]. To test whether PKC and JNK activation were involved in melanomagenesis induced by activated NRAS as modeled *in vitro* [9], we isolated primary melanocytic cells from neonatal skin and at different stages of tumoral progression from *Tyr::NRas*; Pax3*$^{GFP/+}$ mice. pPKCα/β$_{II}$, pJNK and pSTAT3 were analysed by immunofluorescence. Phosphorylation of PKCα/β$_{II}$ was detected both in melanocytes and in tumoral cells, independently of their tumoral progression stage. pJNK, instead, started to be observed in

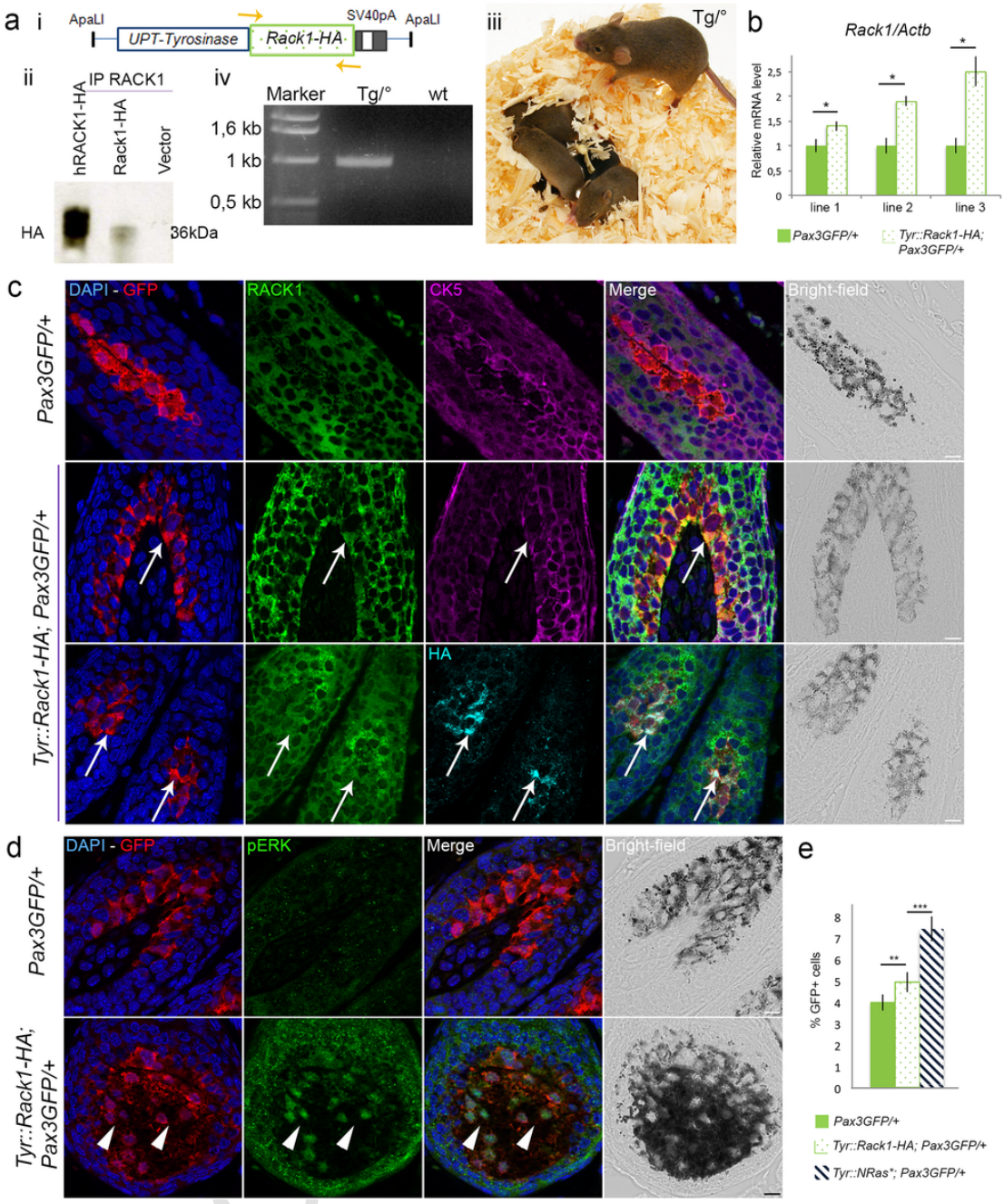

Fig. 3. Targeted RACK1 overexpression in melanocytes is not sufficient to initiate melanoma.a, i Scheme of the *Tyr::Rack1-HA* construct and genotyping strategy (orange arrows), ii Western-blot analysis for HA after RACK1 immunoprecipitation in B16 cells transfected with the above construct and the human RACK1-HA. iii Phenotype of the transgenic mice. iv Detection of the transgene by PCR. b, Reverse transcription-qPCR for *Rack1* RNA in melanocytes isolated by FACS on GFP from *Tyr::Rack1-HA Pax3*$^{GFP/+}$ mice from each of the three transgenic lines (dotted bar) compared to littermates (green bar). Results shown are *Rack1* expression normalized to *Actb* from triplicates. c, ApoTome microscopy analysis of triple labeling for GFP (red), RACK1 (green) and CK5 (magenta) or GFP (red), HA (cyan) and RACK1 (green) in control *Pax3*$^{GFP/+}$ mice and in *Tyr::Rack1-HA; Pax3*$^{GFP/+}$ mice of transgenic line 1. Arrows point to melanocytes overexpressing RACK1. Bar: 10 μm.d, ApoTome microscopy analysis of double labeling for GFP (red) and phospho-ERK (green) in control *Pax3*$^{GFP/+}$ mice and in *Tyr::Rack1-HA; Pax3*$^{GFP/+}$ mice of transgenic line 1. Arrowheads point to melanocytes overexpressing pERK. Nuclear counterstaining in blue. Bars: 10 μm. e, Percentages of GFP cells detected in the dorsal skin of 6 day-old pups from *Pax3*$^{GFP/+}$ (green), *Tyr::Rack1-HA; Pax3*$^{GFP/+}$ (dotted) and *Tyr::NRas*; Pax3*$^{GFP/+}$ (hatched) lines. ** $P < 0.01$, *** $P < 0.001$. (For interpretation of the references to colour in this figure legend, the reader is referred to the web version of this article.)

melanoma cells from primary lesions and was stronger in cells isolated from metastases (Fig. 5a). While no signal was visible on neonatal melanocytes and only a small number of primary cutaneous melanoma cells showed a signal, a high proportion of metastatic cells were found positive for pSTAT3 (Fig. 5a). RACK1 cytoplasmic immunoreactivity instead is detected in all cells (Fig. 5a).

Next, we analysed whether JNK and RACK1 interacted in *Tyr::NRas** melanoma cells. Positive interaction was shown between pJNK and RACK1 by Western blot analysis after RACK1 immunoprecipitation in primary melanoma and metastases. RACK1-pJNK interaction occurred at basal levels, without specific induction suggesting constitutive activation of JNK in these cells (Fig. 5b). We also validated the activation of STAT3 in melanoma cells by Western blot as well as its binding to RACK1, after RACK1 immunoprecipitation. Despite the activation of STAT3 in primary melanoma cells RACK1–pSTAT3 interac-

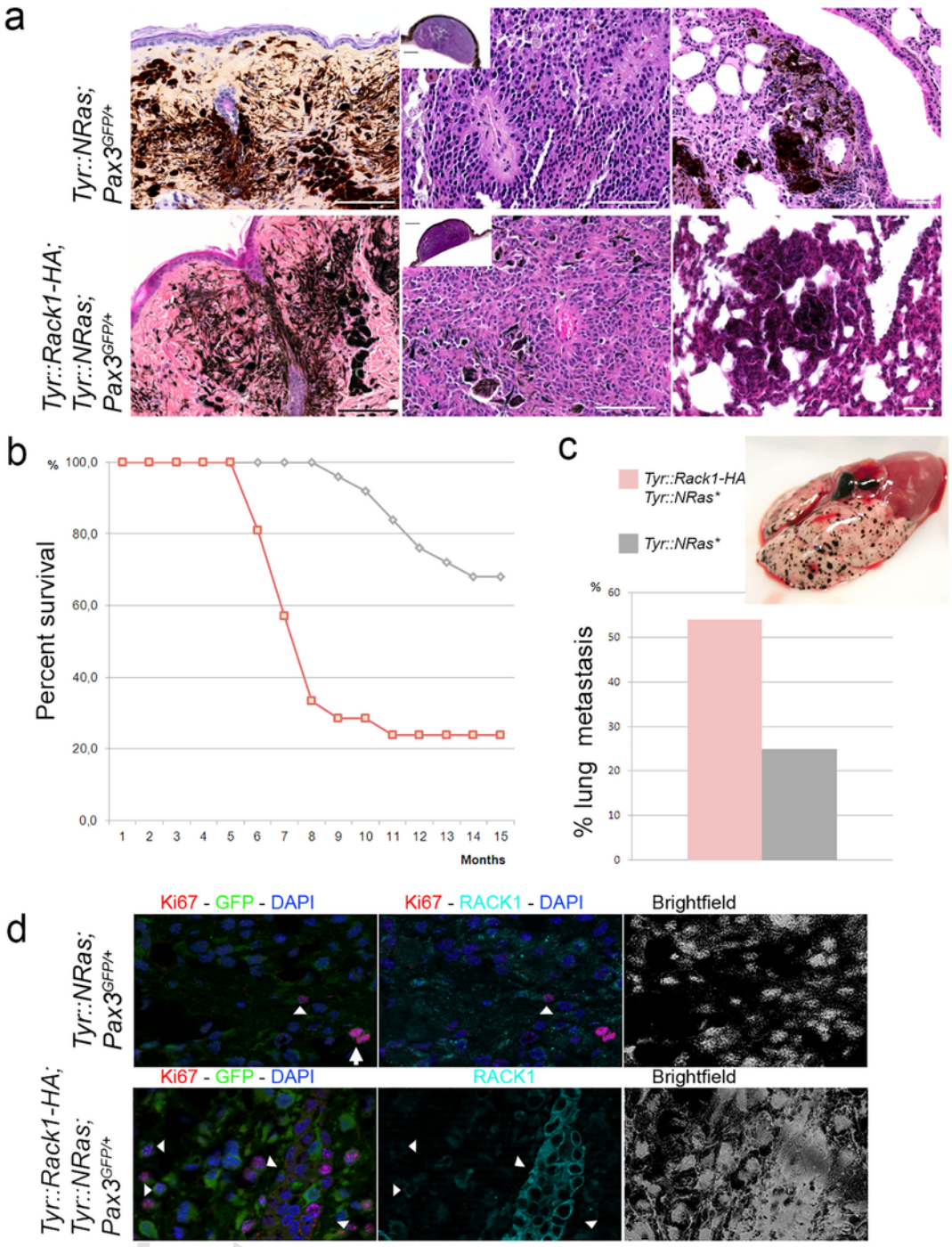

Fig. 4. Targeted RACK1 overexpression reduces latency and increases incidence of melanoma development in *Tyr::NRas** mice.a, Histological features (haematoxylin-eosin-saffron staining) of melanocytic nevi, primary cutaneous melanoma and lung metastases in *Tyr::NRas*; Cdkn2a*$^{+/-}$*; Pax3*$^{GFP/+}$ mice and *Tyr::Rack1-HA; Tyr::NRas*; Cdkn2a*$^{+/-}$*; Pax3*$^{GFP/+}$ mice. Note that lesions are histologically indistinguishable among groups.b, Survival (Kaplan-Meier plot) for *Tyr::Rack1-HA; Tyr::NRas*; Pax3*$^{GFP/+}$ mice (n = 22, pink curve) compared to *Tyr::NRas*; Pax3*$^{GFP/+}$ control mice (n = 25, grey curve). Mice from the three transgenic lines were pooled in the Kaplan-Meier graph.c, Percentages of lung metastases in *Tyr::Rack1-HA; Tyr::NRas*; Pax3*$^{GFP/+}$ mice (pink bar) compared to control *Tyr::NRas*; Pax3*$^{GFP/+}$ (grey bar). Gross feature of a *Tyr::Rack1-HA; Tyr::NRas*; Pax3*$^{GFP/+}$ lung with multiple melanoma metastases.d, ApoTome microscopy analysis of double labeling for Ki67 (red), GFP (green) and RACK1 (cyan) in control *Tyr::NRas*; Pax3*$^{GFP/+}$ mice and in *Tyr::Rack1-HA; Tyr::NRas*; Pax3*$^{GFP/+}$ mice. Nuclear counterstaining in blue. Bars: 10 μm. Arrowheads point to Ki67^{+}, GFP^{+}, RACK1^{+} melanocytic cells. Arrow points to a mitosis, RACK1^{-}. In the lower row, intense RACK1^{+} cells are keratinocytes. (For interpretation of the references to colour in this figure legend, the reader is referred to the web version of this article.)

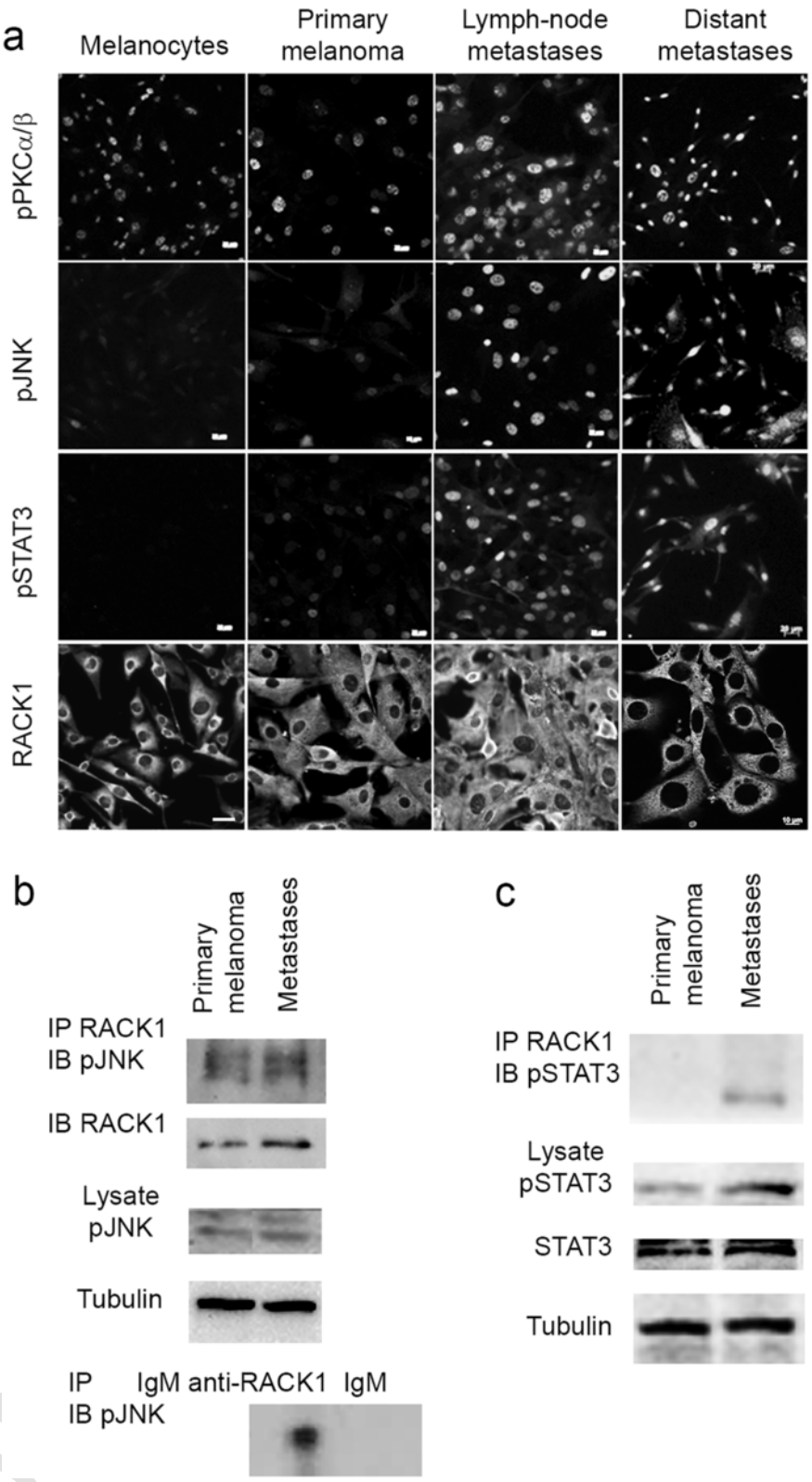

Fig. 5. JNK and STAT3 are oncogenic partners of RACK1 in ERK melanoma development.a, Fluorescent microscopy analysis of immunolabeling for pPKCα/β_{II}, pJNK, pSTAT3 and RACK1 in *Tyr::NRas*; Pax3*$^{GFP/+}$ cells from each stage of melanoma progression. Bars: 10 μm. pPKCα/β_{II} was detected at all stages, pJNK was negative in nontransformed melanocytes and pSTAT3 appeared in metastases.b, Western-blot analysis for pJNK after RACK1 immunoprecipitation in melanoma and lymph node metastases cells. Western blot for pJNK on the 10% inputs used for immunoprecipitation. Below: control immunoprecipitation without RACK1 antibody. Both cell types showed constitutive pJNK-RACK1 interaction.c, Western blot analysis for pSTAT3 after RACK1 immunoprecipitation in lung metastasis cells. Protein interaction between RACK1 and pSTAT3 appears only in metastatic melanoma cells. Western-blot analysis for pSTAT3 and STAT3 in primary melanoma and metastasis cells. Tubulin was used as loading control.

tion was only detected in metastases (Fig. 5c). These data suggest that JNK and STAT3 are activated prior or during the metastatic process.

3.6. Coordinated expression of RACK1, JNK and STAT3 regulates invasive potential

To investigate RACK1, JNK and STAT3 coordination, we verified whether RACK1 levels were under c-Jun transcriptional control treating cells with a JNK inhibitor, SP600125. SP600125 reduced the levels of both 36 kDa and 60 kDa forms of RACK1 in all melanoma cells types (Fig. 6a). A reduction of pJNK was also found (Fig. 6a). When we compared FACS-sorted cells derived from primary melanomas of *Tyr::Rack1-HA; Tyr::NRas*; Pax3$^{GFP/+}$* mice with the ones from *Tyr::NRas*; Pax3$^{GFP/+}$* mice, we observed pJNK immunoreactivity in *Tyr::Rack1-HA* melanoma cells not only in the nucleus but also in the cytosol (Fig. 6b). We reasoned that if RACK1 overexpression accelerated the appearance of tumorigenic properties, a correlation with JNK activity would be found in *Tyr::Rack1-HA* melanoma cells. To test this hypothesis we carried out clonogenic and JNK activity assays. In soft agar assay, cells overexpressing *Rack1* started forming clones earlier than control cells (Fig. 6c). SP600125 treatment of *Tyr::Rack1-HA* melanoma cells prevented colony formation in agar over a 6 days period (Fig. 6c). When immunokinase assays using GST-c-Jun$^{1-89}$ as substrate were performed on primary cells of melanomas, an increased JNK activity was revealed in *Tyr::Rack1-HA* melanoma cells compared to controls *Tyr::NRas** (Fig. 6d). These data point to a stronger JNK activity in RACK1 overexpressing melanomas.

Out of 5 enhancer regions described by ENCODE and identified on human RACK1 genecard (www.genecards.org), three (GHO5E181172, GH05E181215, GH05E181240) present binding sites for STAT3. To test whether STAT3 transcriptionally regulates RACK1 in *Tyr::NRas** cells, we transduced interfering lentiviral *shStat3* vectors. STAT3 knock-down in lung metastasis cells led to *Rack1* mRNA (Fig. 6ei) and RACK1 protein reduction on both the 36 kDa and the 60 kDa bands (Fig. 6eii). *STAT3* knock-down effect on RACK1 mRNA and protein levels was also effective in human UACC903 melanoma cell lines as illustrated in Fig. 6f. As the JNK pathway was shown to activate STAT3 in epithelial cells [21], we tested whether JNK was regulating STAT3 in melanoma cells. In agreement with above findings, pSTAT3 signal was reduced in SP600125-treated mouse cells (Fig. 6a). Inhibition of JNK activation did also reduce STAT3 activation in human melanoma cell lines (Fig. 6g).

In order to further dissect the mechanism engaged by RACK1 overexpression to allow melanoma cells to metastasize, we examined the transcriptome of melanoma cells from primary lesions in *Tyr::NRas** and *Tyr::Rack1-HA, Tyr::NRas** by RNA-seq. Ingenuity Pathway Analysis on numerically differentially expressed genes resulted in the enrichment of tissue morphology, cellular movement, growth and proliferation pathways. *Stat3* appeared increased in *Tyr::Rack1-HA, Tyr::NRas** with a fold change of 1.3. We intended to analyse the effect of *shRack1*. In these heterogeneous primary cultures, estimation of the efficacy of lentiviral vector transduction was around 50% for both *shRack1* and *shScramble* (Fig. 6h). By immunohistochemistry RACK1 protein downregulation was detected in the transduced cells (Fig. 6h) but no reduction of *Rack1* mRNA was noticeable for any of the 6 transcripts of *Rack1*, from which only 2 (ENSMUST00000020640 and ENSMUST00000125166) can be translated. Among the genes that exhibited increased expression in *Tyr::Rack1-HA, Tyr::NRas** cells and decreased expression following *shRack1* treatment, *Adgrg1* encoding the adhesion G protein-coupled receptor G1, has been shown to dually regulate angiogenesis during melanoma progression [22]. Quantitative RT-PCR on *Rack1* exon 2, targeted by the interfering sequence, showed a slight reduction upon *shRack1* treatment (Fig. 6i). Reduction of RACK1 was related to a clear decrease in *Adgrg1* expression in melanoma cells from *Tyr::Rack1-HA, Tyr::NRas** and *Tyr::NRas** mice. The *Adgrg1* reduction was stronger on *Tyr::Rack1-HA, Tyr::NRas** cells, in which *Stat3* reduction was observed, in contrast to *Tyr::NRas** cells (Fig. 6i). In agreement with these results, RACK1 knock-down in B16 cell agar colonies led to pSTAT3 reduction (Fig. 1dii). To test whether angiogenesis could be responsible for the clinical outcome of *Tyr::Rack1-HA, Tyr::NRas** melanomas, we performed α-smooth muscle actin (αSMA) immunofluorescence on the mouse primary melanoma lesions of *Tyr::Rack1-HA, Tyr::NRas** and *Tyr::NRas** models. αSMA is a marker of myofibroblasts and pericytes used to identify capillaries and vascular structures. Fig. 6j shows the higher density of αSMA$^+$ and vascularisation in heavily pigmented lesions in the *Tyr::Rack1-HA* genotype.

4. Discussion

RACK1 overexpression has been described in different solid cancers. Its detection *in situ* was proposed as a diagnostic marker in melanoma [2] and several carcinomas [23–25]. Many studies have shown that RACK1 is involved in multiple aspects of cancer progression *in vitro* (reviewed by [7]). As cell monolayers are far from *in vivo* complexity, we wanted to test whether the model, in which *NRAS^{Q61K}* triggering ERK/c-Jun accumulation with subsequent RACK1 increase and JNK activation, was valid in the mouse. In this study, we generated *Tyr::Rack1-HA* transgenic mice to test a RACK1 role in melanoma initiation and progression *in vivo*. Our results support the model of RACK1 as a major player in melanomagenesis.

We showed that transgenic *Tyr::Rack1-HA* mice overexpressed *Rack1* in melanocytes with concomitant detection of pERK and pAKT. Nevertheless, *Tyr::Rack1-HA* mice did not develop either hyperpigmentation nor melanoma suggesting that additional alterations are required for both events. In *Tyr::NRAS** transgenic mice, *NRAS^{Q61K}* triggers MAPK and PI3K/AKT pathways activation [10]. This mutation leads to hyperproliferation of skin melanocytes and spontaneous melanoma development [11]. We showed here that these mice also overexpress RACK1 in melanocytes. Thus, the difference in phenotypes could be ascribed to a differential compartmentalization of the proteins in the two melanocyte-types engaging then distinct genetic programs [26]. Alternatively, it could hint at the existence of additional pathways triggered by the *NRas^{Q61K}* mutation, independent of ERK, JNK, AKT, STAT3 pathways and scaffold RACK1.

Breeding *Tyr::Rack1-HA* mice with *Tyr::NRAS** mice enhanced melanoma initiation and progression, with reduced latency and increased incidence as well as distant metastases in three independent mouse lines. We provided a first evidence of a role for RACK1 in melanomagenesis *in vivo*.

RACK1 serves as a signaling hub that has been implicated in the regulation of several pathways. To identify proteins mediating a role for RACK1 in melanomagenesis, we determined the activation status of PKCα/β_{II}, STAT3 and JNK in primary cultures. pPKCα/β_{II} was detected since the early stages as described [2], whereas STAT3 and JNK proteins were found activated in all lymph node metastatic cells which are representative of the first metastatic stage. Clinically, improved therapy for melanoma will benefit from understanding the metastatic process at a molecular level. In our primary culture cells, JNK activation marked progression to lymph-node metastases. Fittingly, a pathology study showed JNK activation associated with poor prognosis [27]. However, an oncogenic role of the JNK/c-Jun pathway in melanoma development is still under debate [28]. The tumor suppressor *p16/Cdkn2a* was reported to exert its inhibitory role on tumor cells by suppressing JNK activity [29]. In our system, *Cdkn2a* deletion was not sufficient alone to trigger JNK activation. Lopez-Bergami et al. described that RACK1 mediates JNK activation by PKC *in vitro* [5]. Moreover, in human melanoma cell lines, constitutively active ERK provides signals to increase the activity of JNK *via* a rewired signaling [9]. In the pri-

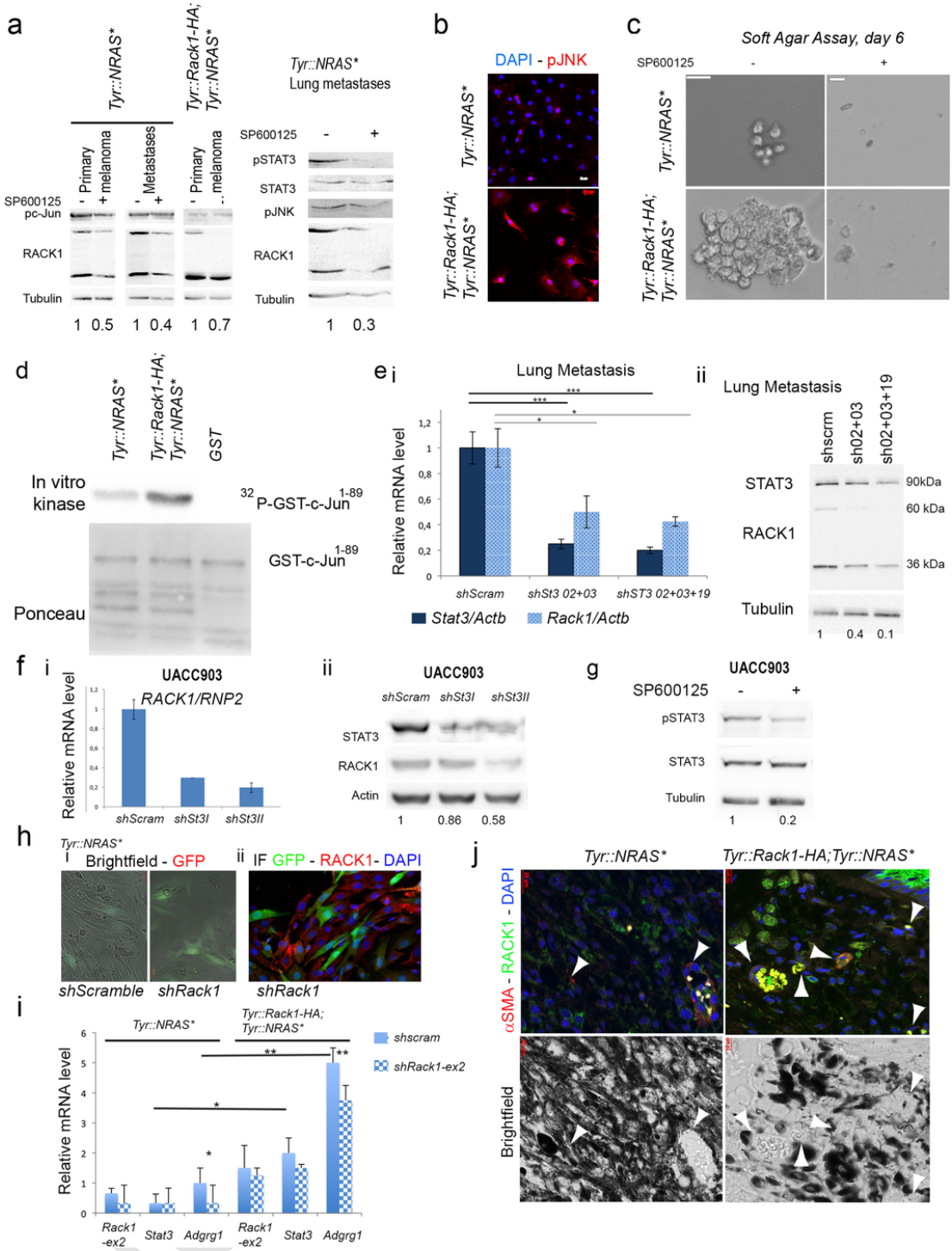

Fig. 6. RACK1 regulation and angiogenesis in melanoma.a, Western blot analysis of pc-Jun and RACK1 after SP600125 inhibition of JNK on protein lysates from primary melanoma and metastases from *Tyr::NRas*; Pax3*$^{GFP/+}$ mice and primary melanoma cells in *Tyr::Rack1-HA; Tyr::NRas*; Pax3*$^{GFP/+}$. SP600125 20 μM reduced RACK1 levels after 48 h treatment. pc-Jun reduction is shown. Western blot analysis of RACK1, pSTAT3, STAT3 and pJNK, in *Tyr::NRas*; Pax3*$^{GFP/+}$ melanoma lung metastatic cells after treatment with 20 μM SP600125 for 48 hs and quantification. b, pJNK immunoreactivity on cells from primary melanomas of *Tyr::Rack1-HA; Tyr::NRas*; Pax3*$^{GFP/+}$ mice compared to the ones from *Tyr::NRas*; Pax3*$^{GFP/+}$ mice. Bars: 10 μm. Note a higher pJNK signal on *Rack1* overexpressing cells.c, Soft agar assay over 6 days with melanoma cells overexpressing *Rack1-HA* and controls without or with SP600125 (20 μM). *Rack1-HA* cells started forming clones earlier, and SP600125 prevented it. Bars: 10 μm.d, *In vitro* JNK kinase assay. Cell lysates from *Tyr::NRas*; Pax3*$^{GFP/+}$ and *Tyr::Rack1-HA; Tyr::NRas*; Pax3*$^{GFP/+}$ melanomas and *Tyr::NRas*; Pax3*$^{GFP/+}$ melanocytes were subjected to immunoprecipitation using JNK antibody followed by kinase assay using GST-c-Jun$^{1-89}$ as substrate.e, i Quantitative RT-PCR for *Stat3* (dark blue bars) and *Rack1* (hatched light bars) mRNAs on lung melanoma metastasis cells after treatment with lentiviral vectors coding for *shStat3* (02, 03, 19) or control. Results shown are *Stat3* or *Rack1* expression normalized to *Actb* from triplicates. * $P < 0.05$, *** $P < 0.001$. ii Western-blot for RACK1, STAT3 and Tubulin after *Stat3* knock-down on mouse melanoma cells.f, i Quantitative RT-PCR for *RACK1* mRNA on human UACC903 melanoma cells after treatment with lentiviral vectors expressing *shSTAT3* or *shScramble*. *RACK1* levels are normalized to *RNP2*. *e*; ii Western-blot for RACK1, STAT3, and Actin after *STAT3* knock-down. g, Western blot analysis for

pSTAT3, STAT3 and Tubulin in human UACC903 cell line after SP600125 treatment. h, i Fluorescent microscopy analysis of GFP signal (red) for infection visualization; ii immunolabeling for RACK1 (green) on *Tyr::NRas*; Pax3$^{GFP/+}$* transducted cells with the *shRack1* lentiviral vector as in Fig. 1.i, Quantitative RT-PCR for *Rack1*, *Stat3* and *Adgrg1* mRNAs on primary melanoma metastasis from *Tyr::Rack1-HA; Tyr::NRas*; Pax3$^{GFP/+}$* or *Tyr::NRas*; Pax3$^{GFP/+}$* mice, after treatment with the lentiviral vector expressing *shRack1*. * $P < 0.05$, ** $P < 0.01$.j, Immunolabeling of αSMA (red) and RACK1 (green) in primary melanoma from *Tyr::NRas*; Pax3$^{GFP/+}$* and *Tyr::Rack1-HA; Tyr::NRas*; Pax3$^{GFP/+}$* mice. Arrowheads point to αSMA$^+$ vascular structures. Bars: 10 μm. Brightfields show higher vascularisation in *Tyr::Rack1-HA; Tyr::NRas*; Pax3$^{GFP/+}$* tissue. (For interpretation of the references to colour in this figure legend, the reader is referred to the web version of this article.)

mary melanoma cells from *Tyr::Rack1-HA; Tyr::NRas*; Pax3$^{GFP/+}$* mice, pJNK was detected both in the nucleus and cytoplasm. JNK activity was increased as determined in the kinase assay. Although we have not explored the underlying mechanism of JNK activation, our data support the previous *in vitro* model where JNK activation is being driven by PKC, ERK and RACK1. Data are consistent with the positive correlation observed between cytoplasmic pJNK and pERK in human melanomas [27], where RACK1 is overexpressed [2]. Phospho-STAT3 on Ser705 was mainly found in lymph-node metastatic cells, which is consistent with progressive activation found in human melanoma cell lines [20] [30] and in tumor samples. In melanoma cells, activated STAT3 was reported to sustain expression of the anti-apoptotic genes, *Bcl-xL* (*Bcl2-like 1*) and *Mcl-1* (*Myeloid cell leukemia sequence 1*) [31]. Constitutive STAT3 activation might be a crucial event in metastasis development. We identified STAT3 as a direct RACK1 partner in melanoma development. Confirming the functional interaction between STAT3 and RACK1 we found that RACK1 was regulated at the mRNA level by STAT3. Noteworthy, STAT3-mediated maintenance of NF-κB activity occurs in human A2058 melanoma cell line [32]. In turn, NF-κB is known to upregulate the transcription of RACK1 through direct interaction with its promoter thus contributing to cell survival in PC12 cells [33]. Besides, inhibition of JNK activity led to decreased activation of STAT3. This was reported in colon cancer cells after treatment with AS601245, another JNK inhibitor [34].

B16 mouse melanoma cells harbor both STAT3 activation and JNK activation (data not shown). RACK1 silencing in B16 cell line led to reduced invasive capacities and cell differentiation and loss. The differentiated shape with dendritic extensions closely resembles the *in situ* status of melanocytes in normal skin where no RACK1 is detected [2,3]. Yet, our results seem to be in apparent contradiction with the recent publication of Marubashi et al. which showed that *Rack1* knock-down in melan-a cells decreased their dendricity [35]. In fact, this specific phenotype corresponded to forskolin treated cells, and it might depend upon the extent of RNA silencing and the time before observation. Previous observations showed that mouse fibroblast cells with silenced RACK1 contained more and longer focal adhesions [18,19].

We observed an additional 60 kDa band revealed by RACK1 antibody only in transformed cells, which does not appear in the literature. This band decreased in the presence of the JNK inhibitor or STAT3 knock down suggesting it could reflect a form of RACK1 related to malignancy. Further investigation must be carried out to understand the significance of this isoform.

RNA-seq data were produced in order to determine the targets of signaling pathways induced by RACK1 overexpression that cause the phenotype changes between normal and tumoral melanocytes with different potential. *Tyr::Rack1-HA; Tyr::NRas** primary melanoma cells expressed a higher basal level of *Adgrg1* mRNA. Interestingly, *Adgrg1* has been related to angiogenesis [22] and RACK1 overexpressing melanomas did appear to contain more αSMA$^+$ cells, a marker of angiogenesis. *Adgrg1* activation was recently shown to promote melanoma migration [37]. Melanomas have a high angiogenic potential. These observations are in agreement with early findings on RACK1 expression during angiogenesis [38]. Biological replicates of tumors should be used to formulate new hypotheses on transcriptional targets of RACK1-involving pathways. The wide implication of RACK1 in physiological processes precludes the possibility to directly act on this protein [7]. Identification of RACK1-protein interactions holds the opportunity to develop new therapeutics by the design of peptides interfering with specific binding partners of RACK1 [39,40].

In summary, we demonstrated that RACK1 is implicated in melanomagenesis. RACK1 enhanced melanoma initiation and progression *in vivo*. We propose that activated STAT3 adds to JNK as RACK1 partners in the metastatic process. Specific interference between RACK1 and its partners must be further analysed as a potential therapeutic improvement in melanoma treatment.

Supplementary data to this article can be found online at http://dx.doi.org/10.1016/j.cellsig.2017.03.015.

Authors contributions

JJP, GEM designed the study, CC performed all studies on the mouse and mouse cell assays, MEP and PLB on human cell lines and the JNK assay, SL, PS performed mouse transgenesis, FB and ERG scored histological samples, JEz performed immunofluorescence, PHC carried out FACS, SP, UM provided lentiviral vectors expressing sh*Rack1*, GAH advised with constructs, DE, performed RNA-seq, JE bioinformatic analysis, EB converted gene names. CC and GEM wrote the manuscript.

Uncited reference

[36]

Acknowledgements

We wish to thank A. Casanova and C. Koenen for dedicated animal husbandry. We are grateful to A. Champeix and P. Wattier for sample inclusions in paraffin. We thank S. Bibi for technical help with qPCR. We thank Pierre Adenot (Microscopie et Imagerie des Microorganismes, Animaux et Aliments, MIMA2, INRA) for access to confocal microscopy facilities. We are thankful to Z. Ronaï for control plasmid used in preliminary experiments. We specially thank A. Eychene and N. Mach for helpful discussions and D. Milan for support. This work was funded by grants from Institut National de la Recherche Agronomique, INRA Crédits incitatifs du département de génétique animale (GEM), l'Agence Nationale de la Recherche Emergence Bio ANR 09-EBIO-006-01 to GEM, Ecos-Sud to JJP, GEM and PLB and Association pour la Recherche contre le Cancer (grants 99/7468 and 1002) to GAH and GEM. CC received a grant (Allocation de Recherche MENRT) from the Ministère de la Recherche et de l'Enseignement Supérieur. MEP received a grant from the CONICET.

References

[1] P.A. Ascierto, S. Agarwala, G. Botti, A. Cesano, G. Ciliberto, M.A. Davies, S. Demaria, R. Dummer, A.M. Eggermont, S. Ferrone, et al., Future perspectives in melanoma research: meeting report from the "Melanoma Bridge". Napoli, December 1st–4th 2015, J. Transl. Med. 14 (2016) 313.

[2] G. Egidy, S. Julé, P. Bossé, F. Bernex, C. Geffrotin, S. Vincent-Naulleau, V. Horak, X. Sastre-Garau, J.J. Panthier, Transcription analysis in the MeLiM swine model identifies RACK1 as a potential marker of malignancy for human melanocytic proliferation, Mol. Cancer 7 (2008) 34.

[3] C. Campagne, S. Julé, F. Bernex, M. Estrada, G. Aubin-Houzelstein, J.J. Panthier, G. Egidy, RACK1, a clue to the diagnosis of cutaneous melanomas in horses, BMC Vet. Res. 8 (2012) 95.

[4] C. Campagne, S. Julé, C. Alleaume, F. Bernex, J. Ezagal, S. Château-Joubert, M. Estrada, G. Aubin-Houzelstein, J.J. Panthier, G. Egidy, Canine melanoma diagnosis: RACK1 as a potential biological marker, Vet. Pathol. 50 (2013) 1083–1090.

[5] P. López-Bergami, H. Habelhah, A. Bhoumik, W. Zhang, L.H. Wang, Z. Ronai, RACK1 mediates activation of JNK by protein kinase C [corrected], Mol. Cell 19 (2005) 309–320.
[6] D. Ron, C.H. Chen, J. Caldwell, L. Jamieson, E. Orr, D. Mochly-Rosen, Cloning of an intracellular receptor for protein kinase C: a homolog of the beta subunit of G proteins, Proc. Natl. Acad. Sci. U. S. A. 91 (1994) 839–843.
[7] D.R. Adams, D. Ron, P.A. Kiely, RACK1, a multifaceted scaffolding protein: structure and function, Cell Commun. Signal 9 (2011) 22.
[8] V. Volta, A. Beugnet, S. Gallo, L. Magri, D. Brina, E. Pesce, P. Calamita, F. Sanvito, S. Biffo, RACK1 depletion in a mouse model causes lethality, pigmentation deficits and reduction in protein synthesis efficiency, Cell. Mol. Life Sci. 70 (2013) 1439–1450.
[9] P. Lopez-Bergami, C. Huang, J.S. Goydos, D. Yip, M. Bar-Eli, M. Herlyn, K.S. Smalley, A. Mahale, A. Eroshkin, S. Aaronson, Z. Ronai, Rewired ERK-JNK signaling pathways in melanoma, Cancer Cell 11 (2007) 447–460.
[10] D.C. Bennett, How to make a melanoma: what do we know of the primary clonal events?, Pigment Cell Melanoma Res. 21 (2008) 27–38.
[11] J. Ackermann, M. Frutschi, K. Kaloulis, T. McKee, A. Trumpp, F. Beermann, Metastasizing melanoma formation caused by expression of activated N-RasQ61K on an INK4a-deficient background, Cancer Res. 65 (2005) 4005–4011.
[12] A. Camacho-Hübner, F. Beermann, Increased transgene expression by the mouse tyrosinase enhancer is restricted to neural crest-derived pigment cells, Genesis 29 (2001) 180–187.
[13] C. Campagne, E. Reyes-Gomez, S. Loiodice, S. Gadin, J. Ezagal, F. Bernex, M. Abitbol, A. Louise, F. Beermann, J.J. Panthier, et al., Haplosufficiency of PAX3 for melanoma development in Tyr: NRASQ61K; Cdkn2a −/− mice allows identification and sorting of melanoma cells using a Pax3GFP reporter allele, Melanoma Res. 26 (2016) 12–20.
[14] C. Campagne, E. Reyes-Gomez, M. Battistella, F. Bernex, S. Château-Joubert, H. Huet, F. Beermann, G. Aubin-Houzelstein, G. Egidy, Histopathological atlas and proposed classification for melanocytic lesions in Tyr:: NRas(Q61K); Cdkn2a(−/−) transgenic mice, Pigment Cell Melanoma Res. 26 (2013) 735–742.
[15] M. Mourtada-Maarabouni, L. Kirkham, F. Farzaneh, G.T. Williams, Functional expression cloning reveals a central role for the receptor for activated protein kinase C 1 (RACK1) in T cell apoptosis, J. Leukoc. Biol. 78 (2005) 503–514.
[16] M.E. Avale, P. Faure, S. Pons, P. Robledo, T. Deltheil, D.J. David, A.M. Gardier, R. Maldonado, S. Granon, J.P. Changeux, U. Maskos, Interplay of beta2* nicotinic receptors and dopamine pathways in the control of spontaneous locomotion, Proc. Natl. Acad. Sci. U. S. A. 105 (2008) 15991–15996.
[17] J. Djian-Zaouche, C. Campagne, E. Reyes-Gomez, S. Gadin-Czerw, F. Bernex, A. Louise, F. Relaix, M. Buckingham, J.J. Panthier, G. Aubin-Houzelstein, Pax3(GFP), a new reporter for the melanocyte lineage, highlights novel aspects of PAX3 expression in the skin, Pigment Cell Melanoma Res. 25 (2012) 545–554.
[18] T. Vomastek, M.P. Iwanicki, H.J. Schaeffer, A. Tarcsafalvi, J.T. Parsons, M.J. Weber, RACK1 targets the extracellular signal-regulated kinase/mitogen-activated protein kinase pathway to link integrin engagement with focal adhesion disassembly and cell motility, Mol. Cell. Biol. 27 (2007) 8296–8305.
[19] H.C. O'Donovan, P.A. Kiely, R. O'Connor, Effects of RACK1 on cell migration and IGF-I signalling in cardiomyoctes are not dependent on an association with the IGF-IR, Cell. Signal. 19 (2007) 2588–2595.
[20] T.X. Xie, F.J. Huang, K.D. Aldape, S.H. Kang, M. Liu, J.E. Gershenwald, K. Xie, R. Sawaya, S. Huang, Activation of stat3 in human melanoma promotes brain metastasis, Cancer Res. 66 (2006) 3188–3196.
[21] B. Chen, J. Liu, Q. Chang, K. Beezhold, Y. Lu, F. Chen, JNK and STAT3 signaling pathways converge on Akt-mediated phosphorylation of EZH2 in bronchial epithelial cells induced by arsenic, Cell Cycle 12 (2013) 112–121.
[22] L. Yang, G. Chen, S. Mohanty, G. Scott, F. Fazal, A. Rahman, S. Begum, R.O. Hynes, L. Xu, GPR56 regulates VEGF production and angiogenesis during melanoma progression, Cancer Res. 71 (2011) 5558–5568.
[23] Z. Wang, B. Zhang, L. Jiang, X. Zeng, Y. Chen, X. Feng, Y. Guo, Q. Chen, RACK1, an excellent predictor for poor clinical outcome in oral squamous carcinoma, similar to Ki67, Eur. J. Cancer 45 (2009) 490–496.
[24] X.X. Cao, J.D. Xu, J.W. Xu, X.L. Liu, Y.Y. Cheng, W.J. Wang, Q.Q. Li, Q. Chen, Z.D. Xu, X.P. Liu, RACK1 promotes breast carcinoma proliferation and invasion/metastasis in vitro and in vivo, Breast Cancer Res. Treat. 123 (2010) 375–386.
[25] S. Shi, Y.Z. Deng, J.S. Zhao, X.D. Ji, J. Shi, Y.X. Feng, G. Li, J.J. Li, D. Zhu, H.P. Koeffler, et al., RACK1 promotes non-small-cell lung cancer tumorigenicity through activating sonic hedgehog signaling pathway, J. Biol. Chem. 287 (2012) 7845–7858.
[26] A. Herrero, B. Casar, P. Colón-Bolea, L. Agudo-Ibáñez, P. Crespo, Defined spatiotemporal features of RAS-ERK signals dictate cell fate in MCF-7 mammary epithelial cells, Mol. Biol. Cell 27 (2016) 1958–1968.
[27] K. Jørgensen, B. Davidson, V.A. Flørenes, Activation of c-jun N-terminal kinase is associated with cell proliferation and shorter relapse-free period in superficial spreading malignant melanoma, Mod. Pathol. 19 (2006) 1446–1455.
[28] P. Lopez-Bergami, The role of mitogen- and stress-activated protein kinase pathways in melanoma, Pigment Cell Melanoma Res. 24 (2011) 902–921.
[29] B.Y. Choi, H.S. Choi, K. Ko, Y.Y. Cho, F. Zhu, B.S. Kang, S.P. Ermakova, W.Y. Ma, A.M. Bode, Z. Dong, The tumor suppressor p16(INK4a) prevents cell transformation through inhibition of c-Jun phosphorylation and AP-1 activity, Nat. Struct. Mol. Biol. 12 (2005) 699–707.
[30] M. Sakaguchi, M. Oka, T. Iwasaki, Y. Fukami, C. Nishigori, Role and regulation of STAT3 phosphorylation at Ser727 in melanocytes and melanoma cells, J. Invest. Dermatol. 132 (2012) 1877–1885.
[31] G. Niu, T. Bowman, M. Huang, S. Shivers, D. Reintgen, A. Daud, A. Chang, A. Kraker, R. Jove, H. Yu, Roles of activated Src and Stat3 signaling in melanoma tumor cell growth, Oncogene 21 (2002) 7001–7010.
[32] H. Lee, A. Herrmann, J.H. Deng, M. Kujawski, G. Niu, Z. Li, S. Forman, R. Jove, D.M. Pardoll, H. Yu, Persistently activated Stat3 maintains constitutive NF-kappaB activity in tumors, Cancer Cell 15 (2009) 283–293.
[33] D.S. Choi, H. Young, T. McMahon, D. Wang, R.O. Messing, The mouse RACK1 gene is regulated by nuclear factor-kappa B and contributes to cell survival, Mol. Pharmacol. 64 (2003) 1541–1548.
[34] A. Cerbone, C. Toaldo, S. Pizzimenti, P. Pettazzoni, C. Dianzani, R. Minelli, E. Ciamporcero, G. Roma, M.U. Dianzani, R. Canaparo, et al., AS601245, an anti-inflammatory JNK inhibitor, and clofibrate have a synergistic effect in inducing cell responses and in affecting the gene expression profile in CaCo-2 colon cancer cells, PPAR Res. 2012 (2012) 269751.
[35] S. Marubashi, N. Ohbayashi, M. Fukuda, A Varp-binding protein, RACK1, regulates dendrite outgrowth through stabilization of Varp protein in mouse melanocytes, J. Invest. Dermatol. 136 (2016) 1672–1680.
[36] X.J. Yang, S. Grégoire, A recurrent phospho-sumoyl switch in transcriptional repression and beyond, Mol. Cell 23 (2006) 779–786.
[37] N.Y. Chiang, Y.M. Peng, H.H. Juang, T.C. Chen, H.L. Pan, G.W. Chang, H.H. Lin, GPR56/ADGRG1 activation promotes melanoma cell migration via NTF dissociation and CTF-mediated Gα12/13/RhoA signaling, J. Invest. Dermatol. (2016).
[38] H. Berns, R. Humar, B. Hengerer, F.N. Kiefer, E.J. Battegay, RACK1 is up-regulated in angiogenesis and human carcinomas, FASEB J. 14 (2000) 2549–2558.
[39] K.J. Smith, G.S. Baillie, E.I. Hyde, X. Li, T.M. Houslay, A. McCahill, A.J. Dunlop, G.B. Bolger, E. Klussmann, D.R. Adams, M.D. Houslay, 1H NMR structural and functional characterisation of a cAMP-specific phosphodiesterase-4D5 (PDE4D5) N-terminal region peptide that disrupts PDE4D5 interaction with the signalling scaffold proteins, beta-arrestin and RACK1, Cell. Signal. 19 (2007) 2612–2624.
[40] M. Kiely, D.R. Adams, S.L. Hayes, R. O'Connor, G.S. Baillie, P.A. Kiely, RACK1 stabilises the activity of PP2A to regulate the transformed phenotype in mammary epithelial cells, Cell. Signal. (2016).